ACS Energy LETTERS

http://pubs.acs.org/journal/aelccp

Stainless Steel Felt as a Combined OER Electrocatalyst/Porous Transport Layer for Investigating Anion-Exchange Membranes in Water Electrolysis

Binyu Chen, Ana Laura G. Biancolli, Chase L. Radford, and Steven Holdcroft*

Cite This: *ACS Energy Lett.* 2023, 8, 2661−2667

Read Online

ACCESS | Metrics & More | Article Recommendations | Supporting Information

ABSTRACT: **Anion-exchange membrane water electrolysis (AEMWE) is a promising technology for low-cost, high-efficiency, green hydrogen production. The stability of the AEM is a critical issue but difficult to delineate *in situ* from degradation of the catalyst layer (CL). Moreover, the porous transport layer (PTL) can contribute electrocatalytically. Herein, we demonstrate that stainless steel (SS) felt, in the absence of an anode CL, is highly active toward the oxygen evolution reaction (OER) (1 A cm^{-2} at 1.74 V_{cell}) and serves as a combined OER electrocatalyst and PTL, thus simplifying the study of AEMs in water electrolyzers. We further show that Ni felt exhibits much lower OER activity than SS felt, which suggests that *in situ* studies of OER electrocatalysts and CL compositions should be performed with Ni felt, not SS felt, to reduce OER contributions from the PTL. Lastly, we found that the substrate for depositing the cathode CL, AEM, or PTL strongly influences the rate of H_2 crossover.**

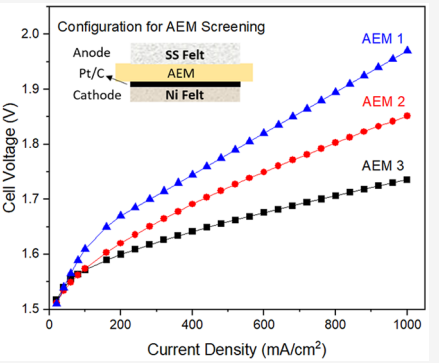

Water electrolysis using renewable electricity is a sustainable technology for clean hydrogen. Conventional alkaline water electrolysis (AWE) is typically operated over a small dynamic window (0.2−0.4 A cm^{-2}) at 60−80 °C with a cell voltage between 1.8 and 2.4 V, limited by the cell's high internal resistance.[1−3] Proton-exchange membrane water electrolysis (PEMWE) technology aims to counter this with its high efficiency, high current densities, and a compact footprint.[4] The acidic environment of PEMWE requires precious-metal electrocatalysts, Ti-based bipolar plates, and porous transport layers (PTLs) stabilized with oxidation-resistant coatings. Collectively, these components significantly increase costs, which limits large-scale commercialization of PEMWE technology.[5] Anion-exchange membrane water electrolysis (AEMWE) technology combines the favorable attributes of both AWE and PEMWE and allows low-cost materials to be used in conjunction with an anion-exchange membrane (AEM).[6,7]

Although AEM water electrolyzers have progressed, there is a distinct lack of comparability/standardization within the field. Only a limited number of cell durability analyses are reported (see Table S1),[8−14] and most studies report different membrane-electrode assembly (MEA) architectures, catalyst layer (CL) compositions, and membranes. The CL in particular plays a major role in the performance and durability of AEM water electrolyzers.[6,15] To limit interfacial resistances, MEAs are typically fabricated by deposition of the CL directly onto the membrane to form a catalyst-coated membrane (CCM).[16,17] Due to the harsh oxidative conditions at the anode, carbon supports for OER electrocatalysts are avoided; this renders CL preparation challenging due to unstable catalyst ink dispersions.[18] Furthermore, CLs typically employ a solubilized anion-exchange ionomer as the ionomer/binder and are highly susceptible to deterioration, detachment, and delamination.[9,19,20] The absence of a thorough understanding of catalyst inks adversely affects the reproducibility and comparability of AEMWE studies, and avoiding CCM preparation typically leads to more robust AEM water electrolyzers.[12,13] For the purpose of developing AEMs for their use in AEMWE, a simple, reproducible, and cost-effective set of baseline materials is needed to deconvolute the

Received: April 30, 2023
Accepted: May 17, 2023
Published: May 22, 2023

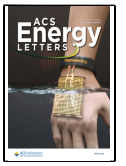

properties of the membrane from the effects of both the nature of the electrocatalyst and the deposition of the CL.

Numerous studies have been conducted on stainless steel (SS) in concentrated alkaline solutions for the application of traditional alkaline water electrolysis,[21−25] but use of SS alone as the anode in AEMWE is rare.[26] In this work, we delineate AEM studies of the effects of the anode CL from the influence of the AEM. We show that SS felt serves as a robust and efficient PTL/OER electrocatalyst for studying AEMs in water electrolyzers, as exemplified in Scheme 1. We also demonstrate

Scheme 1. Illustration of Membrane-Electrode Assemblies (MEAs) of Anode Configurations Studied[a]

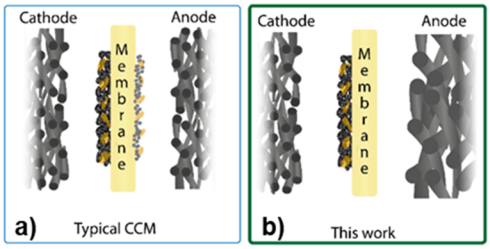

[a](a) Catalyst-coated membrane (CCM). (b) This work, Ni or NiCr or SS felt as OER electrocatalyst/PTL. The cathode comprises Ni felt and CL (Pt/C catalyst + ionomer) coated on the membrane.

that Ni felt has low electrocatalytic activity, and *in situ* studies of novel OER electrocatalysts are better performed with Ni felt, not SS felt, to avoid OER contributions.

Keeping the cathode composition constant (Pt/C/ionomer/Ni felt), we study and compare the influence of three different anode PTL materials (SS felt, NiCr felt, and Ni felt, purchased from Dioxide Materials), with and without an Ir electrocatalyst. Their properties and composition (determined by SEM-EDX) are detailed in Table 1, from which it appears they were made

Table 1. Properties of Porous Transport Layers (PTLs) Employed

PTL	Fiber diameter (μm)	Porosity[a] (%)	Composition[b] (wt %)			
			Ni	Cr	Fe	O
NiCr felt	12	75	69.6	21.6	2.3	0
Ni felt	12	75	97.5	0	0	0.4
SS felt	25	78	9.4	17.4	67.7	0.5

[a]Estimated by density. [b]Analyzed by SEM-EDX.

from stainless steel 304, Inconel 600, and pure nickel, respectively. The details of AEMs are listed in Table 2. The AEMs are chosen to possess a wide variation in membrane properties (composition, functional groups, water uptake, ionic conductivity, and adhesion) to assess a single membrane-electrode-assembly design. Where the Ir OER electrocatalyst is used, as indicated in the figure legend, Ir particles were coated onto the AEM (comprising 90 wt % Ir black, 10 wt % ionomer) with a loading of 3.5 ± 0.2 mg_{Ir} cm^{-2}; the MEA architectures are also shown in the figure legends. For all experiments, Ni felt was used as the cathode PTL, and the H_2 evolution was electrocatalyzed by a CL (comprising 80 wt % Pt/C + 20 wt % ionomer) with a loading of 1.0 ± 0.1 mg_{Pt} cm^{-2} (directly coated onto the AEM, unless specified). Baseline electrocatalysts (Ir at anode and Pt/C at cathode) were chosen in this work as the most commonly adopted electrocatalysts, due to their performance and widespread availability, serving as a suitable reference material. Anion-exchange ionomer (same type of material as AEM, where possible) was used in the CL to minimize catalyst delamination, and the details can be found in Table 2. The single cell/electrolyzer (as shown in Scheme S1) was compressed using eight bolts at a torque of 10 in-lb, and a dual-channel peristaltic pump was used for the 1 M KOH supply (fed to both anode and cathode at a flow rate of 5 mL min^{-1}). Compressible polyolefin gaskets (QuinTech) were used for sealing, and the active area of the MEA was 5 cm^2. The electrolyzer was conditioned at 50 °C, and $I-V$ curves were obtained at 60 °C. Through-plane ionic conductivity was measured using a cell and protocol reported previously;[27] details (cell conditioning, water uptake, materials, MEA fabrication, etc.) can be found in the Supporting Information.

To observe the influence of a given PTL in the absence of a specific OER electrocatalyst, AF1-HNN8-50 AEM was employed in order to compare the results with our previously published AEMWE study using NiCr felt and an Ir CL.[20] As shown in Figure 1a, using NiCr felt as a combined PTL and electrocatalyst, a higher voltage for a given current density was required than when an Ir catalyst is present, consistent with the known OER activity of Ir.[30] Replacing NiCr felt with SS felt alone enhances the electrochemical performance significantly, achieving a similar polarization curve to NiCr felt with Ir CL. Conversely, when replacing NiCr felt with Ni felt, a dramatic reduction in the electrocatalytic activity is found, requiring >2 V to achieve 1000 mA cm^{-2}. These results show that SS felt is highly OER active, and Ni felt is relatively inactive. To analyze the electrode kinetics, we used HFR data from Figure 1b, and iR correction was performed (Figure S1), in order to minimize contact and ionic resistances. As shown in Figure S1, OER activity follows the trend: Ir > SS felt > NiCr felt > Ni felt. Note that while NiCr felt showed modest electrocatalytic activity, SEM-EDX analysis before and after conditioning confirmed substantial oxidation and leaching of Cr, as shown in Figure S2; NiCr felts were therefore excluded from further studies due to uncertainty of the effect of leached ions.

To confirm that the SS felt was not membrane-specific, reinforced polyimidazolium AEM, Aemion AF2-HWP8-75-X, was examined in the same cell configurations. The same trend in polarization curves with anode type was observed, as shown in Figure 1b, where SS felt is highly active (1.72 V at 1000 mA cm^{-2}) and Ni felt is less active (2.09 V at 1000 mA cm^{-2}). A CCM comprised of an Ir CL and an SS or Ni felt shows similar activity (~1.85 V at 1000 mA cm^{-2}), both less active than SS felt alone.

We compared the polarization curves (Figure S3) obtained with the Aemion AEMs AF1-HNN8-50 and AF2-HWP8-75-X; MEAs were prepared with SS felts alone as the anode or using Ir with the corresponding ionomer (indicated in Table 2). Without Ir CLs, AF1- and AF2-based MEAs show similar $I-V$ characteristics. However, with an Ir CL, AF2-MEAs require an additional 130 mV to achieve 1000 mA cm^{-2} despite observing anode catalyst delamination in both cases. As shown in Figure S4, the Ir CL was washed away from the AEM and/or transferred to the PTL, highlighting the need to delineate CL degradation from membrane degradation.

The resistances of AEMWE cells were determined by EIS. As illustrated in Figure 1c,d, from the onset of the semicircles, Ni felt and SS felt exhibit a significantly lower high-frequency

https://doi.org/10.1021/acsenergylett.3c00878
ACS Energy Lett. 2023, 8, 2661−2667

Table 2. Properties of Various Anion-Exchange Membranes and Ionomers Employed

AEM	AEM polymer	Catalyst layer ionomer[a]	Dry thickness (μm)	Water uptake (wt %)[b]	Cl^- conductivity (mS cm^{-1})[b]
Aemion AF1-HNN8-50	polybenzimidazolium	AF1-HNN8-50	50	63 ± 2	6.8 ± 0.1
Aemion AF2-HWP8-75-X	PEEK reinforced polyimidazolium	AP2-HNN8-00-X	85	42 ± 5	4.5 ± 0.2
Aemion AF3-HWK9-75-X	PEEK reinforced polyimidazolium	AP3-HNN9-00	75	43 ± 1	5.4 ± 0.3
Fumasep FAA-3-PK-75	PEEK reinforced proprietary hydrocarbon	FAA-3-SOLUT-10	75	15 ± 1	0.5 ± 0.0[c]
RG-LDPE-37[28,29]	LDPE backbone containing covalently bonded benzyltrimethylammonium head-groups	AF1-HNN8-50	37	51 ± 4	13.6 ± 0.5
RG-LDPE-62[28,29]		AF1-HNN8-50	62	45 ± 1	11.8 ± 0.5

[a]Same material as AEM, where possible. FAA-3-SOLUT is 10 wt % FAA-3 in NMP. Other ionomers were dissolved in methanol (2 wt %) before use. [b]AEM was in its Cl^- form and measured in DI water at ~20 °C; see Supporting Information for experiment details. [c]4.5−6.5 mS cm^{-1} (product data sheet, unknown temperature). Lower values here might be due to the anisotropy.

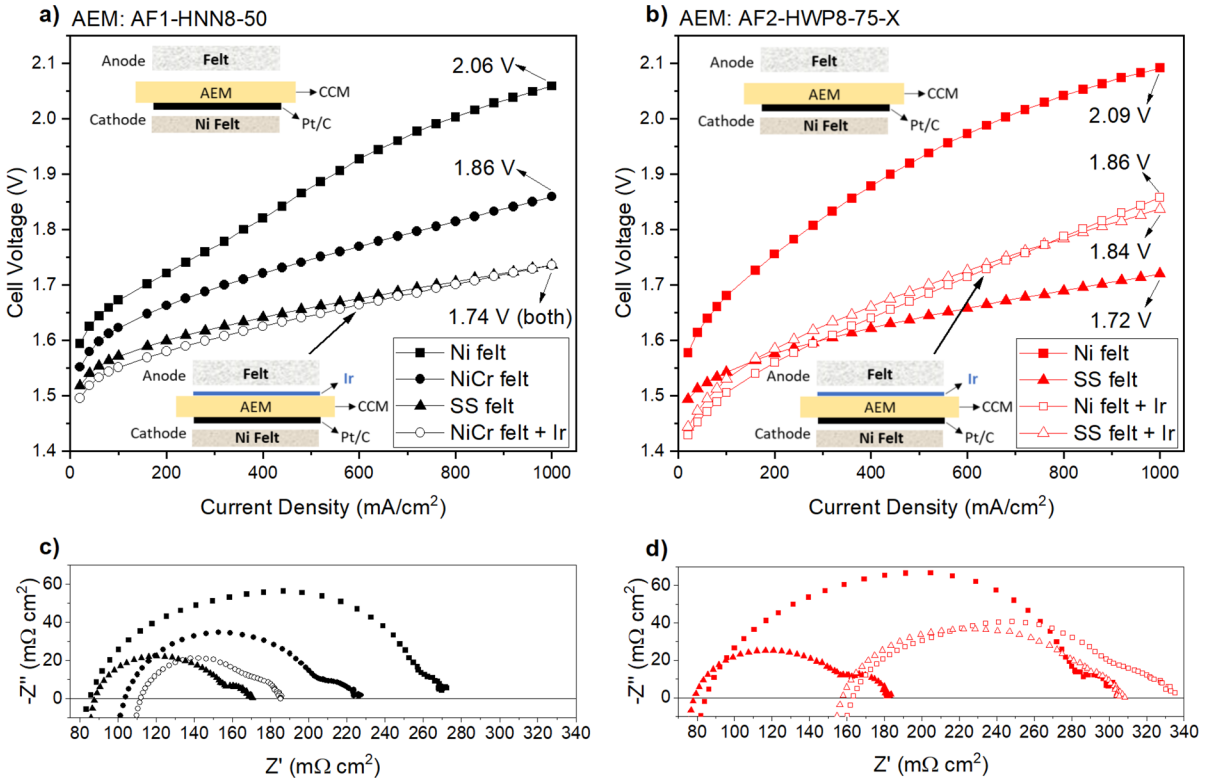

Figure 1. Effect of anode PTL on (a,b) AEMWE polarization curves and (c,d) corresponding Nyquist plots at 600 mA cm^{-2}. Aemion AEMs were used. (a,c) AF1-HNN8-50; (b,d) AF2-HWP8-75. The anode comprised either NiCr felt, NiCr felt and 3.5 mg cm^{-2} Ir (CCM, comprising 90 wt % Ir and 10 wt % ionomer), Ni felt, or SS felt. In all instances, the cathode comprised Ni felt and a CL (CCM, 80 wt % Pt/C catalyst + 20 wt % ionomer). Catalyst layer ionomer: AF1-HNN8-50 and AP2-HNN8-00-X for AF1-HNN8-50 and AF2-HWP8-75-X AEMs, respectively. All experiments were conducted in 1 M KOH at 60 °C with a flow rate of 5 mL min^{-1}; further details are provided in the SI. The solid lines are simply to guide the eye.

resistance than when an Ir CL is included, due to the lower electrical resistance of the pristine metal felts.[31] A smaller semicircle diameter associated with MEAs fabricated with Ir CLs (NiCr felt + Ir), as shown in Figure 1c, is indicative of a lower charge-transfer resistance;[32] this is consistent with the high OER activity of Ir. The offsetting electrical resistance vs charge-transfer resistance leads to similar electrocatalytic activity of MEAs based solely on SS felt and MEAs with Ir CLs (i.e., NiCr felt + Ir), as shown in Figure 1a. For MEAs fabricated with the AEM AF2-HWP8-75-X, Nyquist plots of MEAs containing an Ir CL exhibit a large high-frequency resistance, as observed in Figure 1d, manifested as a large semicircle; this further confirms the detachment of the Ir CL containing the corresponding AP2-HNN8-00-X ionomer.

Four-day chronopotentiometry was conducted on MEAs incorporating AF2-HWP8-75-X AEM and SS felt, Ni felt, and Ir CCMs with Ni and SS felts. Voltage−time plots are shown in Figure 2 for current holds of 600 mA cm^{-2}. In the absence of Ir catalyst, the cell voltage increased rapidly in the first 10 h (Figure 2a) before reaching a plateau, which we believe is due to the decreased surface area (due to leaching) and/or the formation of surface oxides (see Figure S5 for SEM images and EDX analyses of the SS and Ni felts and additional discussion in the Supporting Information). The SS felt showed the highest stabilized OER activity (i.e., constant voltage, ~1.72

https://doi.org/10.1021/acsenergylett.3c00878
ACS Energy Lett. 2023, 8, 2661−2667

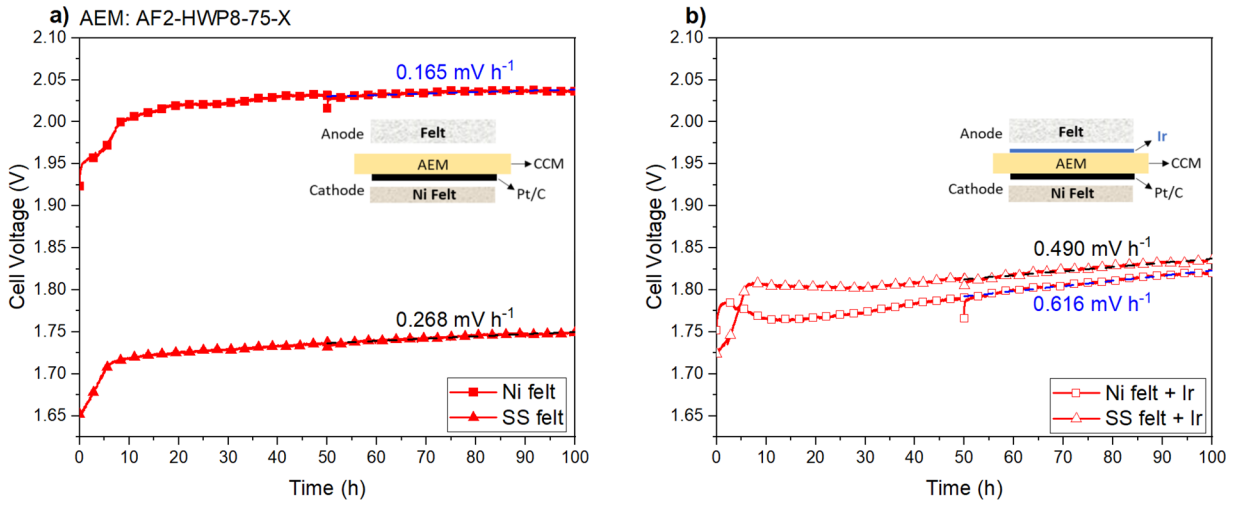

Figure 2. Four-day durability analyses of AEM water electrolyzers at 600 mA cm^{-2}. AEM: Aemion AF2-HWP8-75-X. (a) The anode comprised either Ni felt or SS felt without any CL. (b) The anode comprised a CL containing 3.5 mg cm^{-2} Ir (CCM, 90 wt % Ir + 10 wt % ionomer) and Ni felt or SS felt. The cathode comprised Ni felt and a CL (CCM, 80 wt % Pt/C catalyst + 20 wt % ionomer). AP2-INN8-00-X was used as the ionomer. Experiments conducted in 1 M KOH at 60 °C with a flow rate of 5 mL min^{-1}. The solid lines are simply to guide the eye.

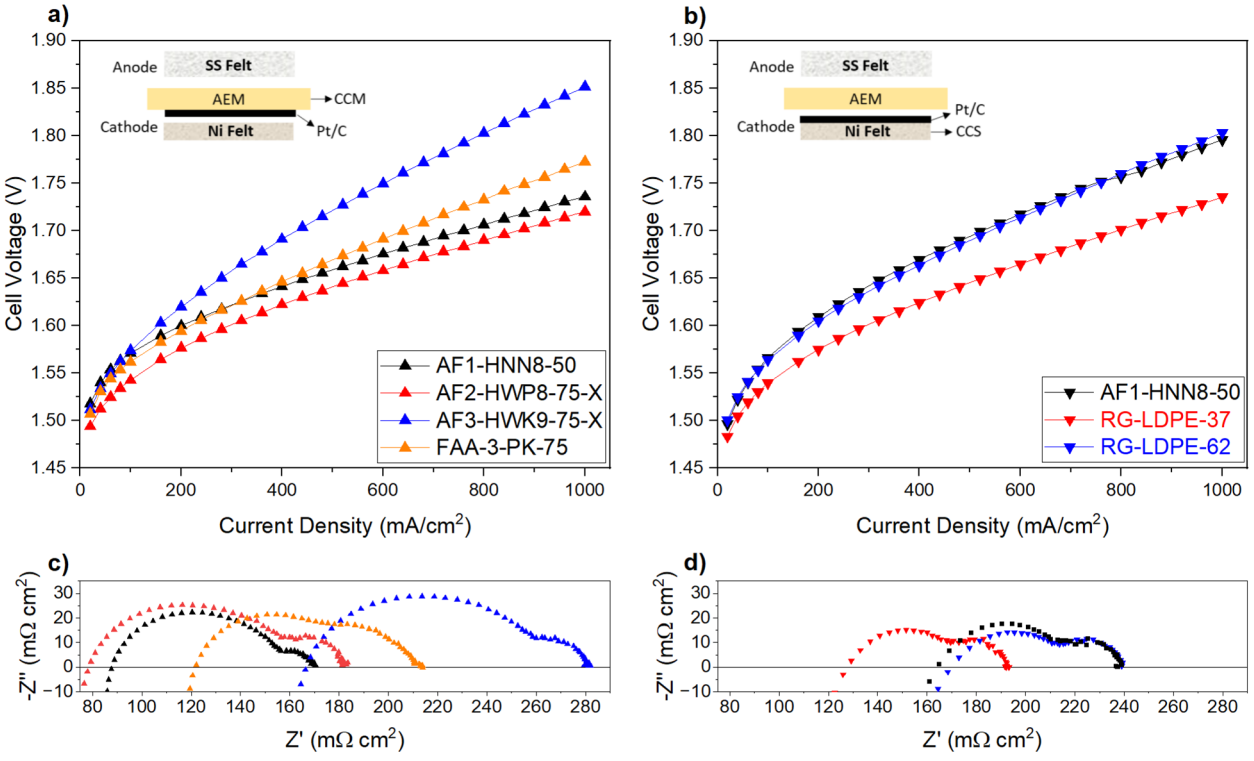

Figure 3. AEM study using an SS felt as an OER electrocatalyst and PTL in an AEM water electrolyzer. (a,b) Polarization curves and (c,d) Nyquist plots at 600 mA cm^{-2}. Anode: SS felt only. Cathode: Pt/C (80 wt % catalyst and 20 wt % ionomer) coated on AEM (CCM) for (a,c) or on the Ni felt (CCS) for (b,d). Different CL ionomers were used according to the AEM type. Experiments were conducted in 1 M KOH at 60 °C with a flow rate of 5 mL min^{-1}. The solid lines are simply to guide the eye.

V). The rate of voltage increase was slightly higher for SS felt than with Ni felt after 50 h (0.268 vs 0.165 mV h^{-1}, respectively), indicating Ni felt is more stable. MEAs with Ir exhibited a higher rate of voltage increase after 50 h than for the MEAs without Ir (0.490 and 0.616 mV h^{-1}, for Ir + SS felt and Ir + Ni felt, respectively) (Figure 2b). This is most likely due to a gradual loss of contact between the anode CL and the AEM, as transfer of catalyst to the PTL is visually observed upon deconstruction of the cell (shown in Figure S4). The higher stability of the AEMs without Ir shows that anode CL delamination greatly interferes with AEM performance and stability studies.

The stability and activity of the SS felt as a combined OER electrocatalyst and PTL removes the variability and irreproducibility of anode CL deposition and delamination, for the purposes of investigating different AEMs. To demonstrate this,

https://doi.org/10.1021/acsenergylett.3c00878
ACS Energy Lett. 2023, 8, 2661−2667

we compared AEMs *in situ* (listed in Table 2): Aemion AEMs, Fumasep AEM, and radiation-induced grafted low-density polyethylene (LDPE)-based AEMs.[28,29] As shown in Figure 3a, polarization curves (using SS felt acting as a combined OER electrocatalyst and PTL) illustrate different $I-V$ characteristics, and the performance implies that membrane hydroxide conductivity (in 1 M KOH at 60 °C) follows: AF1 ≈ AF2 > FAA-3 > AF3 AEMs. EIS spectra (Figure 3c) confirm the trend of membrane hydroxide conductivity, with AF3 showing a much larger high-frequency resistance (170 mΩ cm^2) than AF1 (90 mΩ cm^2), AF2 (80 mΩ cm^2), FAA-3 (120 mΩ cm^2). These results also revealed that the AF1-based MEA has the lowest charge-transfer resistance (70 mΩ cm^2), and the AF3-containing MEA has the largest charge-transfer resistance (90 mΩ cm^2, estimated from the difference between the low-frequency and high-frequency intercepts of the Nyquist plots). Of note, while a typical CCM (Figure 1) showed AF1-based MEA to have the highest performance at high current densities, in the absence of an Ir CL (Figure 3a), AF2-based MEA performs marginally better.

Although lower contact resistance is generally observed with CCMs,[17] some membranes may be less suitable for CCM fabrication due to poor ionomer/membrane compatibility. For example, radiation-induced grafted LDPE AEMs may exhibit poor adhesion with CLs containing ionomers with different compositions (Figure S6: Both anode and cathode CLs detached from AEM (CCM) when soaked in 1 M KOH). The reductive environment at the cathode in AEMWE allows carbon-supported catalysts, which are simpler and more reproducible to spray coat. As shown in Figure 3b,d, the polarization curves and EIS spectra of AF1 and two LDPE-based radiation-grafted AEMs (RG-LDPE-37 and RG-LDPE-62) using SS felt (anode) and Pt/C-coated Ni felt (cathode) showcase the effect of different AEMs, allowing for comparable analyses.

Contemporary AEMWE reports do not routinely report H_2 crossover. By using the methodology demonstrated here, H_2 crossover properties of different AEMs could be readily evaluated without complication of the added anode catalyst layers. As shown in Figure S7, the trend of H_2 crossover is found: AF3 < AF2 < AF1, which is correlated to membrane properties (e.g., thickness, water uptake, and ion-exchange capacity). Moreover, we were able to investigate the impact of depositing the cathode CL on the membrane versus depositing the CL on the cathode PTL (i.e., CCM vs CCS) on the hydrogen crossover rate. We found that the substrate for depositing the cathode CL, either AEM (CCM) or PTL (CCS), plays a large role on the rate of H_2 crossover. As shown in Figure 4, a CCM-based MEA has 2.5 times higher H_2 crossover than a CCS-based MEA. As gas crossover rates are known to be gas flow rate dependent, further studies with variable parameters are warranted.

In summary, we show the influence of the PTL on the OER and demonstrate how it blurs interpretation of the effect of the AEM. We show that stainless steel felt is highly active toward OER, comparable to Ir/ionomer CLs, but without the instability of CLs under the OER conditions. We recommend the PTL should be judiciously chosen depending on what component is being studied and provide two MEA research guidelines: (1) The high electrocatalytic activity and stability of stainless steel felt provides an opportunity to eliminate the Ir catalyst for the purpose of evaluating AEMs. This reduces MEA fabrication time, removes variables between MEA fabrication techniques, reduces screening costs of new materials, and provides a standardized and reproducible MEA architecture that enables more accurate comparisons between the relative merits of AEMs. (2) Ni felt is less OER active than SS felt, which renders Ni felt more suitable for *in situ* studies of electrocatalyst and catalyst layer research. These findings provide AEMWE research a route to comparable and reproducible studies.

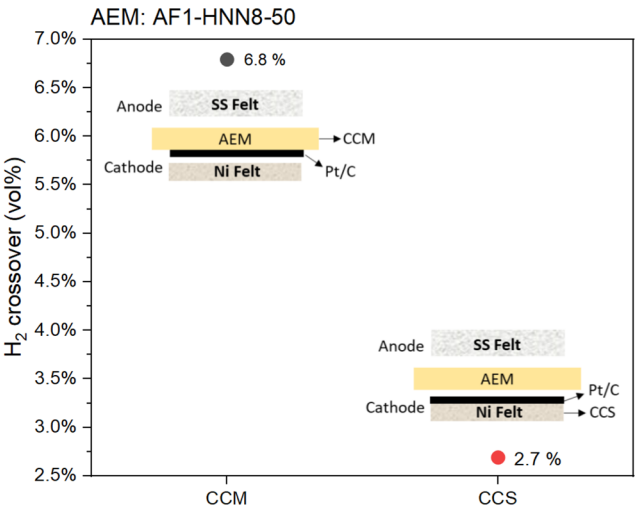

Figure 4. Effect of cathode CL fabrication method (CCM vs CCS) on H_2 crossover. Anode: SS felt only. Cathode: Pt/C (80 wt % catalyst and 20 wt % ionomer) coated on AEM (CCM) or on the Ni felt (CCS). AF1-HNN8-50 was used as ionomer and membrane. Experiments were conducted in 1 M KOH at 60 °C with a flow rate of 5 mL min^{-1}. A constant current of 3 A (0.6 A cm^{-2}) was held for 30 min, and anode gas was collected in a 1 L Tedlar gas sampling bag. H_2 crossover was measured with an Agilent 990 Micro GC. Further details can be found in the SI.

■ ASSOCIATED CONTENT

Supporting Information

The Supporting Information is available free of charge at https://pubs.acs.org/doi/10.1021/acsenergylett.3c00878.

Experimental details, AEMWE literature comparison, SEM-EDX analyses, polarization curves, photographs for visualization of catalyst delamination (PDF)

■ AUTHOR INFORMATION

Corresponding Author

Steven Holdcroft − *Department of Chemistry, Simon Fraser University, Burnaby V5A 1S6, Canada;* orcid.org/0000-0002-1653-1047; Email: holdcrof@sfu.ca

Authors

Binyu Chen − *Department of Chemistry, Simon Fraser University, Burnaby V5A 1S6, Canada*

Ana Laura G. Biancolli − *Department of Chemistry, Simon Fraser University, Burnaby V5A 1S6, Canada; Nuclear and Energy Research Institute, IPEN/CNEN, 05508-000 São Paulo, Brazil*

Chase L. Radford − *Department of Chemistry, Simon Fraser University, Burnaby V5A 1S6, Canada*

Complete contact information is available at: https://pubs.acs.org/10.1021/acsenergylett.3c00878

Notes

The authors declare the following competing financial interest(s): SH is co-founder and a scientific advisor for Ionomr Innovations Inc., supplier of the Aemion membranes and ionomers used in this work.

■ ACKNOWLEDGMENTS

This work was supported by the Natural Sciences and Engineering Research Council of Canada (NSERC) through Discovery Grant RGPIN-2018-03698, by the National Research Council Canada through CSTIP Grant INT-008-1, and made use of 4D LABORATORIES shared facilities at SFU. The authors acknowledge Dr. Xin Zhang (4D LABORATORIES) for help with SEM-EDX, Dr. Peter Mardle for useful discussions, and Dr. Simon Cassegrain for help with the artwork. A.L.G.B. acknowledges FAPESP grants No. 2019/26955-3 and 2021/14786-2 and CINE/SHELL (ANP)/FAPESP grant No. 2017/11937- 4.

■ REFERENCES

(1) Carmo, M.; Fritz, D. L.; Mergel, J.; Stolten, D. A Comprehensive Review on PEM Water Electrolysis. *Int. J. Hydrogen Energy* **2013**, *38* (12), 4901−4934.

(2) Vincent, I.; Bessarabov, D. Low Cost Hydrogen Production by Anion Exchange Membrane Electrolysis: A Review. *Renewable and Sustainable Energy Reviews* **2018**, *81*, 1690−1704.

(3) Miller, H. A.; Bouzek, K.; Hnat, J.; Loos, S.; Bernäcker, C. I.; Weißgärber, T.; Röntzsch, L.; Meier-Haack, J. Green Hydrogen from Anion Exchange Membrane Water Electrolysis: A Review of Recent Developments in Critical Materials and Operating Conditions. *Sustain Energy Fuels* **2020**, *4* (5), 2114−2133.

(4) Feng, Q.; Yuan, X. Z.; Liu, G.; Wei, B.; Zhang, Z.; Li, H.; Wang, H. A Review of Proton Exchange Membrane Water Electrolysis on Degradation Mechanisms and Mitigation Strategies. *J. Power Sources* **2017**, *366*, 33−55.

(5) Shirvanian, P.; van Berkel, F. Novel Components in Proton Exchange Membrane Water Electrolyzers (PEMWE): Status, Challenges and Future Needs. *Electrochem commun* **2020**, *114* (March), 106704.

(6) Santoro, C.; Lavacchi, A.; Mustarelli, P.; di Noto, V.; Elbaz, L.; Dekel, D. R.; Jaouen, F. What Is Next in Anion-Exchange Membrane Water Electrolyzers? Bottlenecks, Benefits, and Future. *ChemSusChem* **2022**, *15* (8), e202200027.

(7) López-Fernández, E.; Sacedón, C. G.; Gil-Rostra, J.; Yubero, F.; González-Elipe, A. R.; de Lucas-Consuegra, A. Recent Advances in Alkaline Exchange Membrane Water Electrolysis and Electrode Manufacturing. *Molecules* **2021**, *26* (21), 6326.

(8) Fortin, P.; Khoza, T.; Cao, X.; Martinsen, S. Y.; Oyarce Barnett, A.; Holdcroft, S. High-Performance Alkaline Water Electrolysis Using Aemion Anion Exchange Membranes. *J. Power Sources* **2020**, *451*, 227814.

(9) Li, D.; Park, E. J.; Zhu, W.; Shi, Q.; Zhou, Y.; Tian, H.; Lin, Y.; Serov, A.; Zulevi, B.; Baca, E. D.; Fujimoto, C.; Chung, H. T.; Kim, Y. S. Highly Quaternized Polystyrene Ionomers for High Performance Anion Exchange Membrane Water Electrolysers. *Nat. Energy* **2020**, *5* (5), 378−385.

(10) Chen, P.; Hu, X. High-Efficiency Anion Exchange Membrane Water Electrolysis Employing Non-Noble Metal Catalysts. *Adv. Energy Mater.* **2020**, *10* (39), 2002285.

(11) Cha, M. S.; Park, J. E.; Kim, S.; Han, S. H.; Shin, S. H.; Yang, S. H.; Kim, T. H.; Yu, D. M.; So, S.; Hong, Y. T.; Yoon, S. J.; Oh, S. G.; Kang, S. Y.; Kim, O. H.; Park, H. S.; Bae, B.; Sung, Y. E.; Cho, Y. H.; Lee, J. Y. Poly(Carbazole)-Based Anion-Conducting Materials with High Performance and Durability for Energy Conversion Devices. *Energy Environ. Sci.* **2020**, *13* (10), 3633−3645.

(12) Wan, L.; Liu, J.; Xu, Z.; Xu, Q.; Pang, M.; Wang, P.; Wang, B. Construction of Integrated Electrodes with Transport Highways for Pure-Water-Fed Anion Exchange Membrane Water Electrolysis. *Small* **2022**, *18* (21), 2200380.

(13) Wan, L.; Xu, Z.; Xu, Q.; Wang, P.; Wang, B. Overall Design of Novel 3D-Ordered MEA with Drastically Enhanced Mass Transport for Alkaline Electrolyzers. *Energy Environ. Sci.* **2022**, *15* (5), 1882.

(14) Kraglund, M. R.; Carmo, M.; Schiller, G.; Ansar, S. A.; Aili, D.; Christensen, E.; Jensen, J. O. Ion-Solvating Membranes as a New Approach towards High Rate Alkaline Electrolyzers. *Energy Environ. Sci.* **2019**, *12* (11), 3313−3318.

(15) Li, D.; Motz, A. R.; Bae, C.; Fujimoto, C.; Yang, G.; Zhang, F.-Y.; Ayers, K. E.; Kim, Y. S. Durability of Anion Exchange Membrane Water Electrolyzers. *Energy Environ. Sci.* **2021**, *14*, 3393.

(16) Lindquist, G. A.; Oener, S. Z.; Krivina, R.; Motz, A. R.; Keane, A.; Capuano, C.; Ayers, K. E.; Boettcher, S. W. Performance and Durability of Pure-Water-Fed Anion Exchange Membrane Electrolyzers Using Baseline Materials and Operation. *ACS Appl. Mater. Interfaces* **2021**, *13* (44), 51917−51924.

(17) Park, J. E.; Kang, S. Y.; Oh, S. H.; Kim, J. K.; Lim, M. S.; Ahn, C. Y.; Cho, Y. H.; Sung, Y. E. High-Performance Anion-Exchange Membrane Water Electrolysis. *Electrochim. Acta* **2019**, *295*, 99−106.

(18) Khandavalli, S.; Park, J. H.; Kariuki, N. N.; Zaccarine, S. F.; Pylypenko, S.; Myers, D. J.; Ulsh, M.; Mauger, S. A. Investigation of the Microstructure and Rheology of Iridium Oxide Catalyst Inks for Low-Temperature Polymer Electrolyte Membrane Water Electrolyzers. *ACS Appl. Mater. Interfaces* **2019**, *11* (48), 45068−45079.

(19) Xiao, J.; Oliveira, A. M.; Wang, L.; Zhao, Y.; Wang, T.; Wang, J.; Setzler, B. P.; Yan, Y. Water-Fed Hydroxide Exchange Membrane Electrolyzer Enabled by a Fluoride-Incorporated Nickel-Iron Oxyhydroxide Oxygen Evolution Electrode. *ACS Catal.* **2021**, *11* (1), 264−270.

(20) Chen, B.; Mardle, P.; Holdcroft, S. Probing the Effect of Ionomer Swelling on the Stability of Anion Exchange Membrane Water Electrolyzers. *J. Power Sources* **2022**, *550* (July), 232134.

(21) Schäfer, H.; Beladi-Mousavi, S. M.; Walder, L.; Wollschläger, J.; Kuschel, O.; Ichilmann, S.; Sadaf, S.; Steinhart, M.; Küpper, K.; Schneider, L. Surface Oxidation of Stainless Steel: Oxygen Evolution Electrocatalysts with High Catalytic Activity. *ACS Catal.* **2015**, *5* (4), 2671−2680.

(22) Anantharaj, S.; Venkatesh, M.; Salunke, A. S.; Simha, T. V. S. V.; Prabu, V.; Kundu, S. High-Performance Oxygen Evolution Anode from Stainless Steel via Controlled Surface Oxidation and Cr Removal. *ACS Sustain Chem. Eng.* **2017**, *5* (11), 10072−10083.

(23) Schäfer, H.; Sadaf, S.; Walder, L.; Kuepper, K.; Dinklage, S.; Wollschläger, J.; Schneider, L.; Steinhart, M.; Hardege, J.; Daum, D. Stainless Steel Made to Rust: A Robust Water-Splitting Catalyst with Benchmark Characteristics. *Energy Environ. Sci.* **2015**, *8* (9), 2685−2697.

(24) Moureaux, F.; Stevens, P.; Toussaint, G.; Chatenet, M. Timely-Activated 316L Stainless Steel: A Low Cost, Durable and Active Electrode for Oxygen Evolution Reaction in Concentrated Alkaline Environments. *Appl. Catal., B* **2019**, *258* (March), 117963.

(25) Zamanizadeh, H. R.; Sunde, S.; Pollet, B. G.; Seland, F. Tailoring the Oxide Surface Composition of Stainless Steel for Improved OER Performance in Alkaline Water Electrolysis. *Electrochim. Acta* **2022**, *424* (May), 140561.

(26) Faqeeh, A. H.; Symes, M. D. A Standard Electrolyzer Test Cell Design for Evaluating Catalysts and Cell Components for Anion Exchange Membrane Water Electrolysis. *Electrochim. Acta* **2023**, *444*, 142030.

(27) Soboleva, T.; Xie, Z.; Shi, Z.; Tsang, E.; Navessin, T.; Holdcroft, S. Investigation of the Through-Plane Impedance Technique for Evaluation of Anisotropy of Proton Conducting Polymer Membranes. *J. Electroanal. Chem.* **2008**, *622* (2), 145−152.

(28) Biancolli, A. L. G.; Barbosa, A. S.; Kodama, Y.; de Sousa, R. R.; Lanfredi, A. J. C.; Fonseca, F. C.; Rey, J. F. Q.; Santiago, E. I. Unveiling the Influence of Radiation-Induced Grafting Methods on the Properties of Polyethylene-Based Anion-Exchange Membranes for Alkaline Fuel Cells. *J. Power Sources* **2021**, *512*, 230484.

https://doi.org/10.1021/acsenergylett.3c00878
ACS Energy Lett. 2023, 8, 2661−2667

(29) Barbosa, A. S.; Biancolli, A. L. G.; Lanfredi, A. J. C.; Rodrigues, O.; Fonseca, F. C.; Santiago, E. I. Enhancing the Durability and Performance of Radiation-Induced Grafted Low-Density Polyethylene-Based Anion-Exchange Membranes by Controlling Irradiation Conditions. *J. Membr. Sci.* **2022**, *659*, 120804.
(30) Tahir, M.; Pan, L.; Idrees, F.; Zhang, X.; Wang, L.; Zou, J. J.; Wang, Z. L. Electrocatalytic Oxygen Evolution Reaction for Energy Conversion and Storage: A Comprehensive Review. *Nano Energy* **2017**, *37*, 136−157.
(31) Kang, Z.; Wang, H.; Liu, Y.; Mo, J.; Wang, M.; Li, J.; Tian, X. Exploring and Understanding the Internal Voltage Losses through Catalyst Layers in Proton Exchange Membrane Water Electrolysis Devices. *Appl. Energy* **2022**, *317* (April), 119213.
(32) Siracusano, S.; Trocino, S.; Briguglio, N.; Baglio, V.; Aricò, A. S. Electrochemical Impedance Spectroscopy as a Diagnostic Tool in Polymer Electrolyte Membrane Electrolysis. *Materials* **2018**, *11* (8), 1368.

https://doi.org/10.1021/acsenergylett.3c00878
ACS Energy Lett. 2023, 8, 2661−2667